Molecular and Cellular Biology

Epigenetic Regulation of Autophagy by the Methyltransferase G9a

Amaia Artal-Martinez de Narvajas, Timothy S. Gomez, Jin-San Zhang, Alexander O. Mann, Yoshiyuki Taoda, Jacquelyn A. Gorman, Marta Herreros-Villanueva, Thomas M. Gress, Volker Ellenrieder, Luis Bujanda, Do-Hyung Kim, Alan P. Kozikowski, Alexander Koenig and Daniel D. Billadeau

Mol. Cell. Biol. **2013, 33(20):3983. DOI: 10.1128/MCB.00813-13.**
Published Ahead of Print 5 August 2013.

MCB
Journals.ASM.org

Epigenetic Regulation of Autophagy by the Methyltransferase G9a

Amaia Artal-Martinez de Narvajas,[a] Timothy S. Gomez,[a] Jin-San Zhang,[a] Alexander O. Mann,[a] Yoshiyuki Taoda,[b] Jacquelyn A. Gorman,[a] Marta Herreros-Villanueva,[a] Thomas M. Gress,[c] Volker Ellenrieder,[c] Luis Bujanda,[d] Do-Hyung Kim,[e] Alan P. Kozikowski,[b] Alexander Koenig,[a,c] Daniel D. Billadeau[a]

Department of Immunology and Division of Oncology Research, Schulze Center for Novel Therapeutics, College of Medicine, Mayo Clinic, Rochester, Minnesota, USA[a]; Department of Medicinal Chemistry & Pharmacognosy, University of Illinois at Chicago, Chicago, Illinois, USA[b]; Department of Gastroenterology and Endocrinology, Philipps University of Marburg, Marburg, Germany[c]; Department of Gastroenterology, Donostia Hospital Biodonostia Institute, Centro de Investigacion Biomedica en Red de enfermedades Hepaticas y Digestivas, Universidad del Pais Vasco, San Sebastian, Spain[d]; Department of Biochemistry, Molecular Biology, and Biophysics, University of Minnesota, Minneapolis, Minnesota, USA[e]

Macroautophagy is an evolutionarily conserved cellular process involved in the clearance of proteins and organelles. Although the cytoplasmic machinery that orchestrates autophagy induction during starvation, hypoxia, or receptor stimulation has been widely studied, the key epigenetic events that initiate and maintain the autophagy process remain unknown. Here we show that the methyltransferase G9a coordinates the transcriptional activation of key regulators of autophagosome formation by remodeling the chromatin landscape. Pharmacological inhibition or RNA interference (RNAi)-mediated suppression of G9a induces LC3B expression and lipidation that is dependent on RNA synthesis, protein translation, and the methyltransferase activity of G9a. Under normal conditions, G9a associates with the LC3B, WIPI1, and DOR gene promoters, epigenetically repressing them. However, G9a and G9a-repressive histone marks are removed during starvation and receptor-stimulated activation of naive T cells, two physiological inducers of macroautophagy. Moreover, we show that the c-Jun N-terminal kinase (JNK) pathway is involved in the regulation of autophagy gene expression during naive-T-cell activation. Together, these findings reveal that G9a directly represses genes known to participate in the autophagic process and that inhibition of G9a-mediated epigenetic repression represents an important regulatory mechanism during autophagy.

Autophagy is an evolutionarily conserved catabolic process in eukaryotes that involves lysosomal degradation of cellular components, including long-lived proteins and organelles. There are four main forms of autophagy: macroautophagy (referred to here as autophagy), selective autophagy, microautophagy, and chaperone-mediated autophagy (1–4). Autophagy serves as an adaptive response to protect cells or organisms during periods of cellular stress, such as nutrient deprivation. In addition, autophagy can participate in several cellular and developmental processes, including homeostasis, clearance of intracellular pathogens, and immunity (1). Due to its fundamental importance for cellular survival, autophagy regulation has been implicated in several human diseases, such as cancer and neurodegenerative disorders (2, 5).

Autophagy initiation involves the *de novo* synthesis of a double-membrane structure known as the phagophore, which ultimately elongates and closes to sequester cytoplasmic proteins and organelles, forming the autophagosome. The autophagosome subsequently undergoes a stepwise maturation process that culminates in its fusion with acidified endosomal/lysosomal vesicles, resulting in the degradation of its contents into useful biomolecules (2). A screen of yeast mutants unable to survive under nitrogen deprivation characterized a network of autophagy-related (ATG) genes (6). Mammalian homologues of these ATGs were later identified and shown to participate during distinct steps of autophagy. For example, microtubule-associated protein light chain 3 (LC3B) undergoes lipidation and is recruited to the phagophore, where it is essential for membrane elongation and closure. Several other proteins are also involved in autophagosome formation, including members of the WD repeat domain phosphoinositide-interacting β-propeller proteins (WIPIs) (7, 8) and the LC3B-interacting protein diabetes and obesity regulated (DOR) (9, 10).

Although the cytoplasmic network leading to autophagy induced by starvation, hypoxia, or receptor stimulation has been widely studied (1–4, 11), the nuclear regulation that initiates and maintains the process remains poorly understood. In fact, while recent publications have just begun to suggest the role of transcription factors such as TFEB (1, 12), E2F1 (1, 2, 13), and FOXO family members (2, 14) in autophagy induction, the epigenetic mechanisms that control chromatin reorganization for transcriptional initiation during autophagy regulation are unknown.

Modifications of histone lysine residues represent one of the major mechanisms in epigenetic regulation of gene expression. Protein lysine methyltransferases (PKMT) catalyze the transfer of methyl groups to distinct lysine residues within histone tails, leading to silencing or activation of target gene promoters. Due to their function in these vital regulatory processes, it is not surprising that there is increasing evidence that specific members of the PKMT family participate in human diseases, especially carcino-

Received 25 June 2013 Returned for modification 12 July 2013
Accepted 24 July 2013
Published ahead of print 5 August 2013

Address correspondence to Daniel D. Billadeau, billadeau.daniel@mayo.edu, or Alexander Koenig, koenigal@med.uni-marburg.de.

A.A.-M.D.N and T.S.G. contributed equally to this work.

Supplemental material for this article may be found at http://dx.doi.org/10.1128/MCB.00813-13.

doi:10.1128/MCB.00813-13

genesis (6, 15). In fact, the methyltransferase G9a, which is ubiquitously expressed in somatic cells, is highly expressed in a variety of human cancers such as leukemia (7, 8, 16, 17) and prostate (9, 10, 18), lung (16), and hepatocellular (19) carcinomas. G9a localizes to euchromatin in a heteromeric complex with G9a-like protein (GLP), a highly homologous methyltransferase. As predicted by its localization, the G9a/GLP complex usually functions to repress gene transcription, especially during embryonic development. In addition, several reports have documented a repressive function for G9a in the expression of rapidly regulated genes (20, 21). This G9a-mediated silencing involves its ability to mono- and dimethylate lysine 9 on histone 3 (16, 17, 22), epigenetic marks that are recognized by the HP1-dependent repressor complex (16, 18, 23). Additionally, G9a/GLP can directly recruit DNA methyltransferases to promoters, resulting in the methylation of CpG islands and gene repression (24, 25).

In the present work, we provide experimental evidence supporting the role of the methyltransferase G9a in the transcriptional regulation of key autophagy-related genes. Pharmacological inhibition or RNA interference (RNAi) of G9a resulted in increased LC3B gene expression and lipidation and increased p62 aggregation. In addition, we demonstrate that G9a associates with the LC3B, WIPI1, and DOR gene promoters and represses gene expression in a methyltransferase-dependent manner. Significantly, during physiological induction of autophagy by glucose starvation or T-cell receptor stimulation of naive T cells, G9a and its repressive histone marks were removed from these promoter loci, resulting in increased gene expression. Taken together, our findings have identified G9a as an epigenetic regulator of autophagy and suggest that inhibition of G9a-mediated gene repression is mechanistically important during the induction of autophagy.

MATERIALS AND METHODS

Reagents and plasmids. Reagents were purchased from Sigma unless otherwise specified. Antibodies against LC3B (catalog no. 3868), p62 (catalog no. 7695), AMPK (catalog no. 5831), pAMPK (T172; catalog no. 2535), ULK1 (catalog no. 4776), pULK1 (S555; catalog no. 5869), and pULK1 (S757; catalog no. 6888) were obtained from Cell Signaling Technology. Antibodies against G9a (catalog no. 3546-1; Epitomics), Atg5 (catalog no. NB110-53818; Novus Biologicals), γ-tubulin (catalog no. T3526; Sigma), and human LAMP1 (catalog no. SC20011; Santa Cruz Biotechnology) were also used. Anti-CD3 (OKT3) was purchased from the Mayo Clinic Pharmacy. Anti-CD28 (catalog no. 555625) and anti-CD69-PE (catalog no. 10450) were from BD Biosciences. Antibodies against histone H3 (dimethyl K9; catalog no. 07-452), histone H3 (acetylation; catalog no. 06-599), RNA polymerase II (catalog no. 05-952), and c-Jun (catalog no. 06-225) were obtained from Millipore. Actinomycin D and rapamycin were from EMD, and annexin V was from eBioscience. UNC0638 was purchased from Sigma. Torin was from Tocris Bioscience, PP2 was from Calbiochem, U0126 was from Promega, and SP600125 was from InvivoGen. The GFP-Cherry-p62 construct was generated using standard molecular biology techniques. Full-length G9a was cloned from a pancreatic cDNA library and used to generate G9aΔSet (encoding amino acids 1 to 971). The short hairpin RNA (shRNA) targeting sequences are available in Table S5 in the supplemental material. G9a cDNA was made resistant to shG9a#2 by mutagenesis and used to generate dual-suppression, hemagglutinin (HA)- and yellow fluorescent protein (YFP)-tagged rescue vectors as described previously (26). All constructs were verified by sequencing in the Gene Analysis Core at Mayo Clinic.

Cell culture, transfection, and stimulation. HeLa and SU86.86 cells were maintained in RPMI, and mouse embryonic fibroblasts (MEFs) were in Dulbecco's modified Eagle medium (DMEM) supplemented with 10% fetal bovine serum (FBS) and 4 mM L-glutamine. For starvation, cells were grown in RPMI medium without glucose (Gibco) supplemented with 1% dialyzed fetal bovine serum (FBS) (Gibco) for 12 to 20 h. Wild-type or Atg5$^{-/-}$ MEFs were grown in DMEM with 10% FBS and 4 mM L-glu-

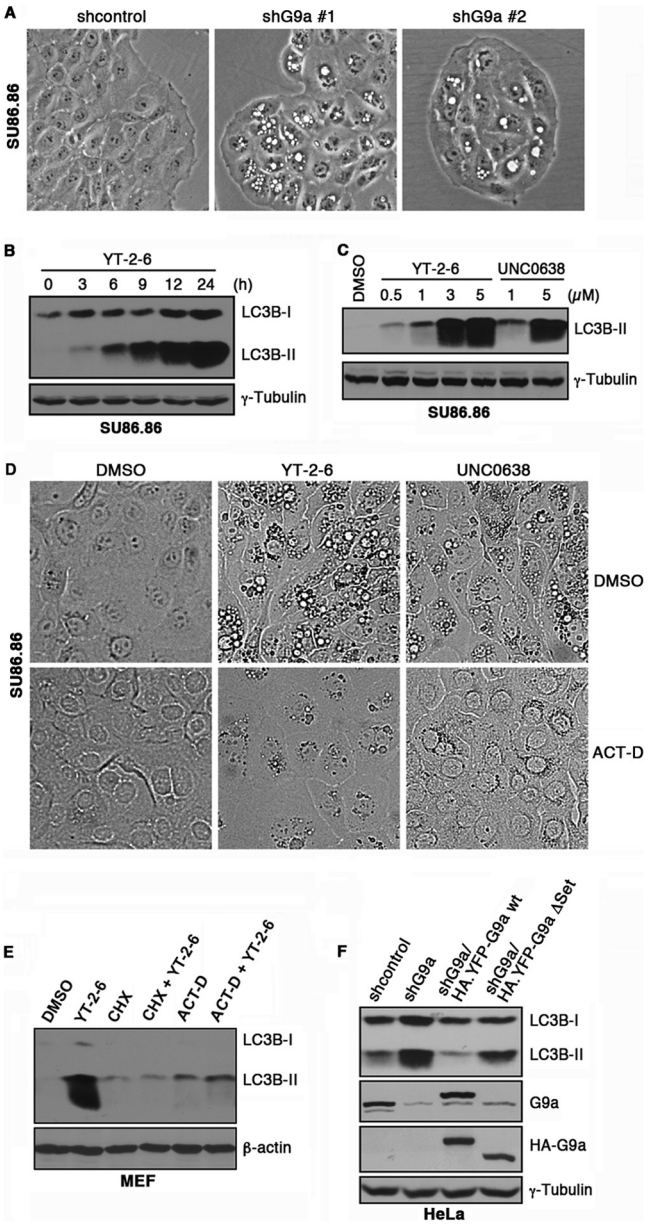

FIG 1 Inhibition or depletion of G9a promotes the formation of vacuole-like structures and increases LC3B-II. (A) Bright-field images of SU86.86 cells depleted of G9a expression show the distinct vacuolar phenotype of enlarged autophagosomes. (B and C) Immunoblot analysis for LC3B expression and lipidation in SU86.86 cells treated with 3 mM YT-2-6 for the indicated times (B) or with the indicated concentrations of YT-2-6 or UNC0638 for 12 h (C). (D) Bright-field analysis of SU86.86 cells treated with diluent, 3 μM YT-2-6, 5 μM UNC0638, and/or 2 μg/ml actinomycin D (ACT-D) for 36 h. (E) Immunoblot analysis for LC3B in MEFs treated with diluent, 3 μM YT-2-6, 20 μg/ml cycloheximide, 2 μg/ml actinomycin D, or the indicated combinations for 24 h. (F) Immunoblot analysis for LC3B in HeLa cells transiently depleted of G9a expression along with reexpression of the wt HA-YFP-tagged G9a or G9a ΔSet domain.

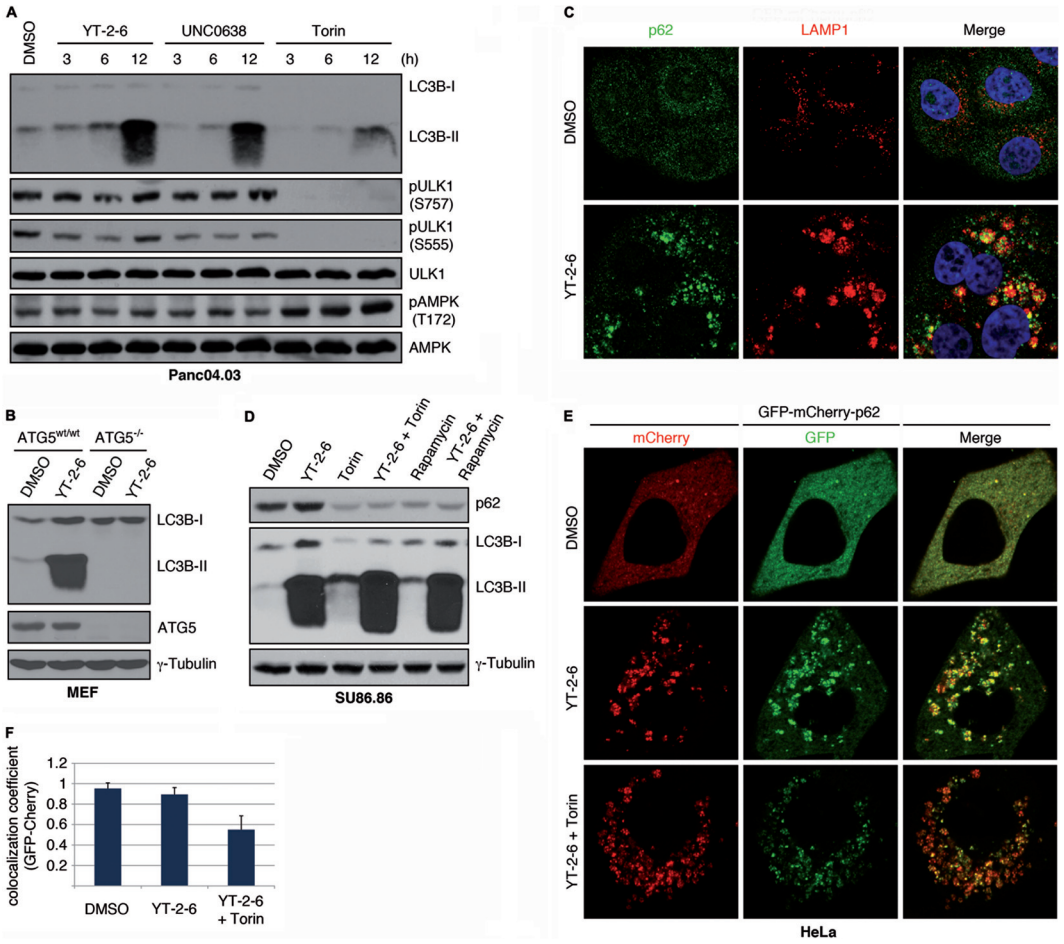

FIG 2 G9a inhibition results in formation of autophagosomes but not autophagic flux. (A) Panc04.03 cells were treated over time with 3 μM YT-2-6, 5 μM UNC0638, or 250 nM torin for 12 h, and lysates were immunoblotted with the indicated antibodies. (B) Immunoblot analysis for LC3B lipidation in ATG5$^{-/-}$ mouse fibroblasts treated with diluent or 3 μM YT-2-6 for 12 h. (C) Pancreatic SU86.86 cells were analyzed by immunofluorescence for LAMP1 (red) along with p62 (green) after treatment with 3 μM YT-2-6 for 12 h. The nucleus was visualized by Hoechst staining (blue). (D) Immunoblot analysis of SU86.86 cells treated for 12 h with a 3 μM concentration of the G9a inhibitor YT-2-6, the TORC inhibitors torin (250 nM) and rapamycin (100 nM), or combinations as indicated shows that although p62 is upregulated upon G9a inhibition, it does not get degraded within autolysosomes unless G9a inhibition is combined with TORC inhibition. (E) Analysis of dually tagged GFP-mCherry-p62 to study autophagic flux in HeLa cells upon treatment with 3 μM YT-2-6 and/or 250 nM torin for 12 h. (F) Colocalization coefficients were determined from the results in panel E for mCherry overlap with GFP (lower colocalization indicates mCherry fluorescence independent of GFP and exposure of the tagged p62 to an acidic compartment).

tamine. HeLa cells were transfected with 25 to 30 μg of plasmid using electroporation (350 V, 1 pulse, 10 ms; BTX Electro Square Porator, ECM830). Primary human T cells were isolated from normal donor peripheral blood using RosetteSep human CD4$^+$ enrichment cocktail (Stemcell Technologies) and were grown in RPMI with 10% FBS and 4 mM L-glutamine. T cells were stimulated with plate-bound anti-CD3 and anti-CD28 (5 μg/ml) for 24 to 48 h.

RNA extraction, cDNA synthesis, qRT-PCR, and profiler. RNA was extracted using the RNeasy minikit from Qiagen. To produce cDNA, 1 μg of total RNA was processed with the Superscript III RT-PCR kit (Invitrogen) according to the manufacturer's instructions. Quantitative PCR (qPCR) was performed using the comparative cycle threshold (C_T) method with SYBR green PCR master mix from Applied Biosystems and the ABI Prism 7900TM sequence detection system. Experiments were performed in triplicate using three independent cDNAs. Primer sequences are presented in Table S3 in the supplemental material. The qRT-PCR autophagy profiler was from Qiagen and analyzed according to the manufacturer's instructions.

Immunoblotting. Cells were lysed with RIPA buffer (1% Triton X-100, 0.5% sodium deoxycholate, 0.1% SDS, 150 mmol/liter NaCl, 50 mmol/liter Tris-HCl [pH 7.2], 10 mmol/liter EDTA, 10 mmol/liter EGTA). Cleared lysates were subjected to SDS-PAGE and immunoblotting using antibodies listed above.

Microscopy and flow cytometry. SU86.86 cells were grown directly on coverslips at 37°C and imaged using a Zeiss Axiovert or Zeiss 710 confocal microscope. For flow cytometry, cells were stained in phosphate-buffered saline (PBS) with 0.5% bovine serum albumin (BSA) with propidium iodide or by using antibodies for CD3, CD4, and CD69 and analyzed using a FacsCanto II with FACSDiva software (BD Biosciences).

Chromatin immunoprecipitation (ChIP). ChIP was performed in naive human CD4$^+$ T cells, isolated from human blood and stimulated with anti-CD3/anti-CD28, and pancreatic cancer cells (SU86.86) using the EZ ChIP kit (Millipore) according to the manufacturer's instructions. Briefly, after treatment or posttransfection, cells were cross-linked and lysed, and DNA was sheared to fragments of 400 to 700 bp by sonication (Bioruptor; Diagenode). Precleared chromatin was immunoprecipitated with the antibodies indicated in the figures, and DNA was isolated after reverse cross-linking for PCR. Primer sequences are presented in Table S4 in the supplemental material.

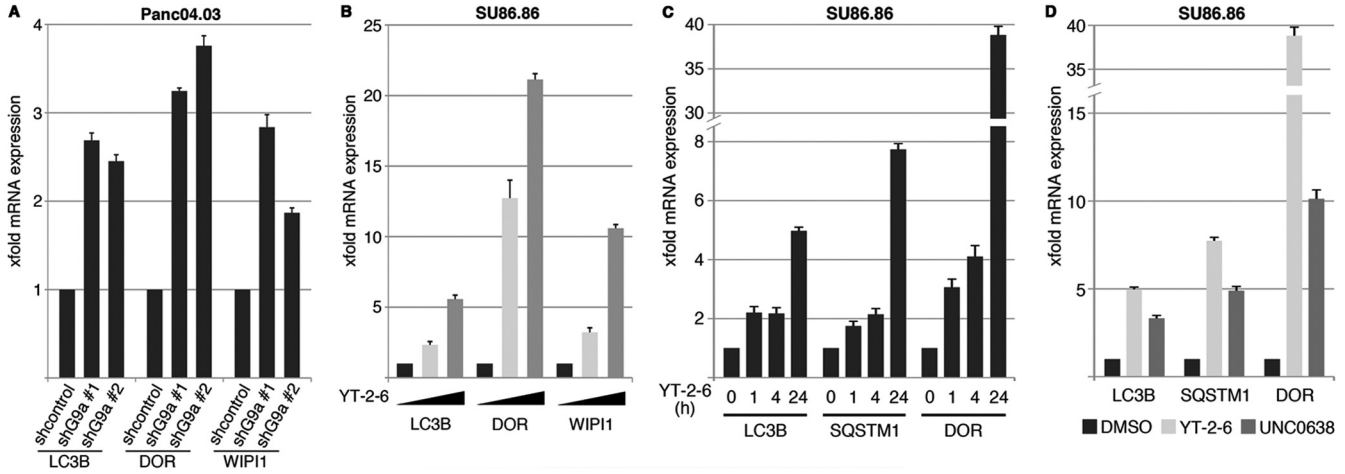

FIG 3 G9a inhibition leads to increased expression of genes involved in autophagosome formation. (A) Quantitative RT-PCR analysis of identified target genes in Panc04.03 cells transiently depleted of G9a expression. (B to D) Quantitative RT-PCR analysis in SU86.86 cells treated with diluent or 3 μM or 5 μM YT-2-6 for 24 h (B), 3 μM YT-2-6 for the indicated times (C), or 3 μM YT-2-6 or 5 μM UNC0638 for 24 h (D). Results were normalized to RPLP0 and are displayed as *x*-fold over the value for controls (mean plus standard deviation [SD]).

RESULTS

Loss of G9a function induces formation of vacuolar structures and increased LC3B-II in a methyltransferase-dependent manner. During investigations examining the effect of G9a inhibition on cancer cell proliferation, we noticed that transfection of cells with shRNA vectors targeting G9a resulted in the formation of large cytoplasmic vacuole-like structures in the pancreatic cancer cell line SU86.86 (Fig. 1A). Biochemically, we noted that depletion of G9a by RNAi in HeLa cells induced LC3B-II formation that could be rescued by reexpression of wild-type G9a (see Fig. S1A and B in the supplemental material). Moreover, treatment with two chemically distinct inhibitors of G9a, YT-2-6 (see Fig. S1C in the supplemental material) and UNC0638 (27) led to the formation of LC3B-II in multiple cell lines in a time- and dose-dependent manner (Fig. 1B; also, see Fig. S1D to F in the supplemental material). In addition, both inhibitors resulted in the formation of vacuolar structures similar to those seen with G9a suppression (Fig. 1D, top). Importantly, the addition of either G9a inhibitor at the concentrations that induced the vacuole-like structures did not induce apoptosis (see Fig. S1G in the supplemental material).

Since G9a functions to methylate histones and regulate gene expression, we investigated whether gene transcription was required for vacuole-like structure and LC3B-II formation following G9a inhibition. Consistent with this idea, inhibition of mRNA synthesis by actinomycin D reduced the characteristic vacuolar phenotype induced upon G9a inhibition and impaired LC3B-I expression as well as the formation of LC3B-II (Fig. 1D, bottom, and 1E). Moreover, new protein synthesis was required, as cycloheximide also prevented induction of LC3B-I protein expression as well as its conversion into LC3B-II following G9a inhibition (Fig. 1E). Additionally, as seen in Fig. 1F, reexpression of wild-type (wt) G9a rescued the effect on LC3B lipidation in G9a-depleted cells, while reexpression of a methyltransferase-deficient G9a mutant (G9aΔSet) failed to prevent LC3B-II formation. Together, these findings suggested that transcriptional control by G9a represents an epigenetic mechanism that governs LC3B-I gene expression and the formation of LC3B-II.

G9a inhibition does not induce autophagic flux in the absence of mTOR inhibition. To determine if autophagosome formation in response to G9a inhibition was dependent upon mTOR or AMPK, the key protein kinases known to regulate autophagy induction (28, 29), we compared the phosphorylation status of ULK1 at Ser757 (mTOR site required for AMPK-ULK1 association) and Ser555 (AMPK site) upon treatment with YT-2-6, UNC0638, or torin (30). Although we observed more LC3B-II upon inhibition of G9a, we observed loss of p-ULK1 for both sites only with torin, not with YT-2-6 or UNC0638. Additionally, AMPK phosphorylation at Thr172, which was previously shown to increase upon mTor inhibition (31), was increased with torin but not G9a inhibitor treatment (Fig. 2A). In order to determine whether autophagosomes induced upon G9a inhibition utilized the canonical pathway for formation, we examined LC3B-II conversion in ATG5-deficient MEFs, a key regulator of this process (32, 33). As shown in Fig. 2B, LC3B-II generation no longer occurred in ATG5-deficient MEFs treated with the G9a inhibitor. Taken together, these data indicate that loss of G9a activity utilized the ATG5-dependent pathway of autophagosome formation but did so independently of mTOR inactivation.

The autophagy adaptor protein involved in recognition of ubiquitinated autophagy substrates, p62 (also known as SQSTM1), forms aggregates, is targeted to the lumen of the autophagosome, and is degraded along with cargos during the completion of autophagy (34). Using confocal microscopy, we investigated whether p62 formed aggregates and localized with lysosomes in response to G9a inhibition. Significantly, G9a inhibition resulted in the aggregation of p62 that partially overlapped LAMP1 (Fig. 2C). We therefore examined p62 levels in order to assess autophagic degradation of p62 following pharmacologic inhibition of G9a. Upon YT-2-6 treatment, we observed a slight but reproducible increase in p62 protein levels, whereas torin or rapamycin treatment led to p62 degradation, indicative of autophagic flux (Fig. 2D). However, when YT-2-6 was cotreated with torin or rapamycin, p62 was degraded (Fig. 2D), suggesting that G9a inhibition alone is insufficient to drive the autophagic process without concomitant inhibition of mTOR.

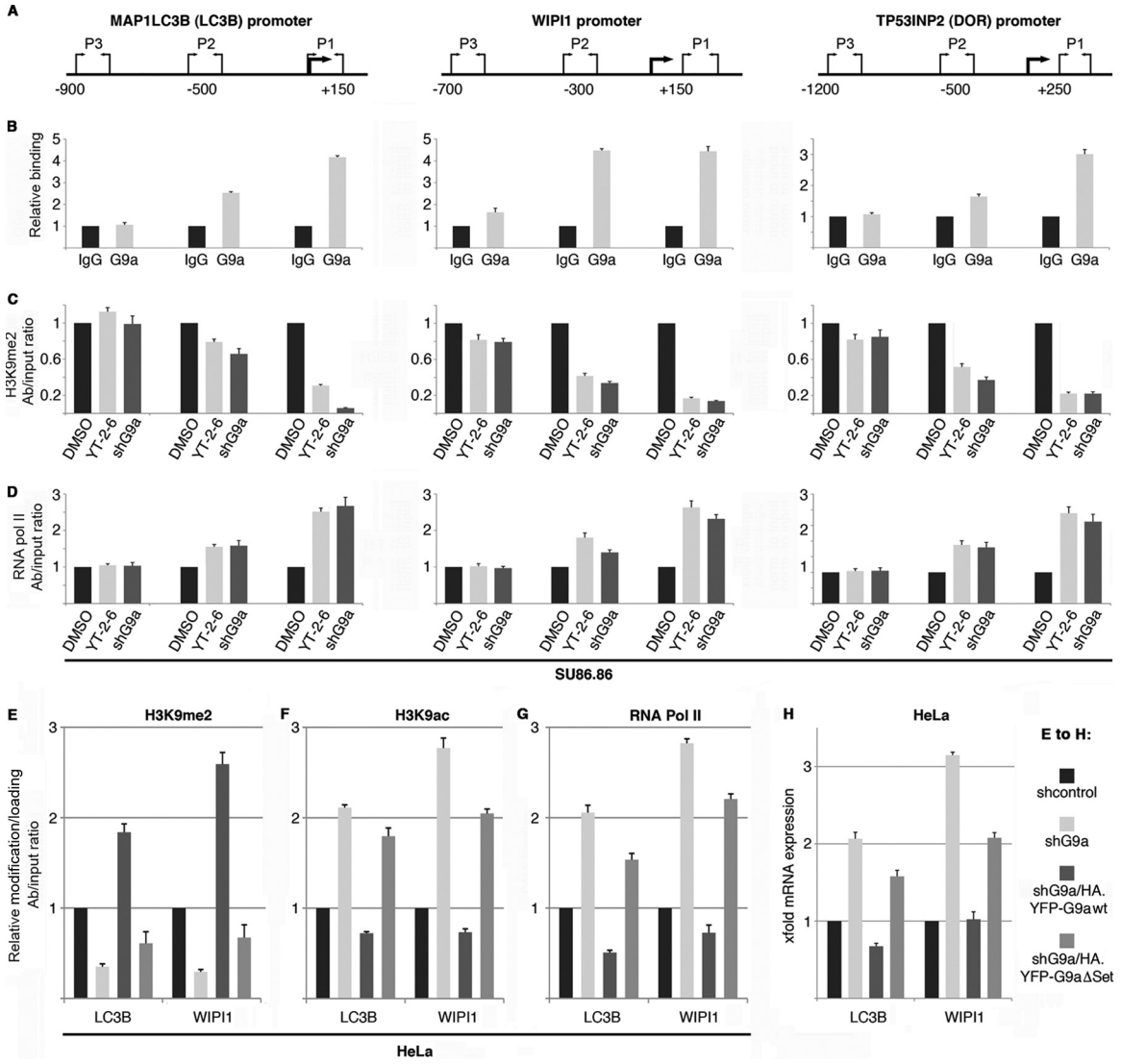

FIG 4 Inhibition or genomic depletion of G9a alters G9a promoter binding and chromatin modifications of genes involved in autophagosome formation. (A) Cartoon of the LC3B promoter showing the localization of the primers (P1 to P3) used for panels B to D, relative to the transcription start (arrow). (B) Quantitative PCR of ChIP analysis shows G9a association with the LC3B, WIPI1, and DOR promoters relative to input and displayed as fold over IgG (mean plus SD) in untreated pancreatic SU86.86 cells. (C and D) Quantitative analysis following ChIP in SU86.86 cells treated with 3 μM YT-2-6 for 24 h or stably depleted of G9a shows H3K9me2 and binding of RNA polymerase II to the LC3B, WIPI1, and DOR promoter relative to input and displayed as fold over the value for control cells (mean plus SD). (E to G) Quantitative ChIP PCR analysis shows H3K9me2 (E), H3K9ac (F), and RNA polymerase II (G) binding to the LC3B promoter. Results are relative to input and displayed as fold over the value for control cells (mean plus SD). Primer P1 (for H3K9me2 and RNA polymerase II [Pol II]) and primer P2 (for H3K9ac) was used to analyze the promoter (see the cartoon in Fig. 2A). (H) Quantitative RT-PCR for LC3B and WIPI1 expression in HeLa cells transfected with the indicated suppression and reexpression constructs for G9a. Results are normalized to RPLP0 and displayed as fold over the value for controls (mean plus SD).

We next examined whether the accumulated p62 entered the acidic autophagosome lumen using a dual-tagged mCherry-GFP-p62 biosensor, an approach previously utilized to examine LC3B autophagic flux (35). Consistent with the observations that G9a inhibition could promote p62 aggregation but was insufficient to promote autophagic flux, we found that GFP-mCherry-p62 aggregated in YT-2-6-treated cells but did not enter the acidic lumen efficiently, since the p62 aggregates contained both mCherry and GFP fluorescence (Fig. 2E) (GFP fluorescence is quenched within the acidic environment of the lysosome). However, consistent with Fig. 2D, dual treatment with YT-2-6 and torin resulted in the entry of p62 into the acidic autolysosome and subsequent p62 degradation (Pearson's colocalization coefficients: for dimethyl sulfoxide [DMSO], 0.96 ± 0.05; for YT-2-6, 0.9 ± 0.07; for YT-2-6 plus torin, 0.55 ± 0.13) (Fig. 2E and F). Taken together, these data suggest that G9a inhibition alone, while sufficient to induce LC3B-II lipidation and p62 aggregation, is insufficient to drive autophagic flux.

G9a regulates the expression of genes involved in autophagosome formation and the process of autophagy. Since our data point to a role for G9a in the epigenetic regulation of LC3B accumulation and lipidation, we decided to determine whether

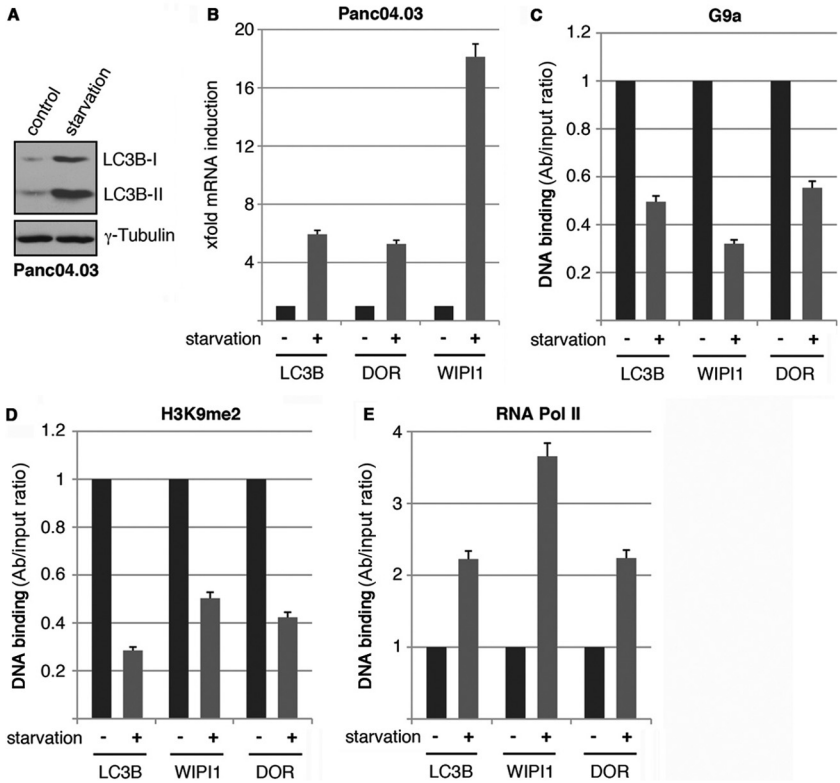

FIG 5 Nutrient starvation, a physiologic stressor which triggers autophagy induction, leads to G9a-dependent, epigenetic changes at autophagy-related target gene promoters. (A) Immunoblot analysis of Panc04.03 cells upon glucose starvation for 18 h shows expression and lipidation of LC3B. (B) Quantitative RT-PCR analysis of selected genes in Panc04.03 cells upon glucose starvation for 18 h. Results were normalized to RPLP0 and are displayed as *x*-fold over the value for controls (mean plus SD). (C to E) Quantitative PCR of ChIP analysis in glucose-starved Panc04.03 cells shows association of G9a (C), H3K9me2 (D), and RNA polymerase II binding (E) to the LC3B, WIPI1, and DOR promoters. Results are relative to input and displayed as fold over the value for control cells (mean plus SD). Primer P1 (see the cartoon in Fig. 4A) was used in ChIP for analyzing all three promoters.

G9a might be involved in the regulation of genes involved in the autophagic process. To identify G9a target genes, we screened the autophagy profiler from Qiagen. Interestingly, G9a inhibition increased expression of LC3B and p62 (3, 36) (see Table S1 in the supplemental material). Other autophagy genes were also upregulated, including ATG9B, GABARAPL1, GABARAPL2, BNIP3, and UVRAG (see Table S1). Additionally, and consistent with our immunoblot results, LC3B mRNA was substantially increased after pharmacological or genetic depletion of G9a (Fig. 3). We also examined the expression of other genes (not present on the autophagy profiler) known to participate in autophagosome formation. Significantly, DOR (diabetes and obesity regulated) and WIPI1, which regulate autophagosome formation in different organisms (7, 9, 10, 37), were significantly upregulated upon depletion of G9a (Fig. 3A). Additionally, inhibition of G9a induced the expression of LC3B, WIPI1, DOR, and p62 in a concentration- and time-dependent manner starting 1 h postinhibition (Fig. 3B to D).

G9a associates with the LC3B, DOR, and WIPI1 promoters. Since LC3B, DOR, and WIPI1 are evolutionarily conserved throughout eukaryotes and participate in autophagosome formation, we focused on these three genes for further analysis. To examine G9a-dependent epigenetic regulation of these genes, we mapped the corresponding target gene promoters for G9a association in chromatin immunoprecipitation (ChIP) experiments (Fig. 4A). We found G9a to be associated with all three target gene promoters in a region near the transcriptional start site (Fig. 4B). Upon G9a inhibition or knockdown, we detected a reduction in G9a-related H3K9me2 and an increase in RNA polymerase II binding at the corresponding sequences (Fig. 4C to G). Importantly, while reexpression of wild-type (wt) G9a in G9a-depleted cells rescued H3K9me2, suppressed H3K9ac (a mark of active gene expression), and decreased RNA polymerase II binding, reexpression of G9aΔSet failed to rescue these chromatin changes at the LC3B and WIPI1 promoters (Fig. 4E to G). Consistent with these G9a-dependent modifications of the chromatin landscape, reexpression of wt G9a in G9a-depleted cells suppressed LC3B and WIPI mRNA expression, while reexpression of G9aΔSet did not (Fig. 4H). Interestingly, recent genome-wide ChIP-sequencing (ChIP-Seq) analysis in *Drosophila melanogaster* following depletion of G9a showed a loss of H3K9me2 at the promoter regions of the homologues of LC3B, DOR, and WIPI1, suggesting that these genes are conserved G9a targets in human and *Drosophila melanogaster* (see Table S2 in the supplemental material) (38). Taken together, these results indicate that direct G9a-dependent chromatin modifications occur at genes involved in autophagosome formation. Nevertheless, analysis of microarray data from G9a-deficient MEFs did not reveal increased expression of these target genes (39). This disparity might be explained by different expression patterns of critical demethylases, which are required to remove methyl marks from these gene promoters.

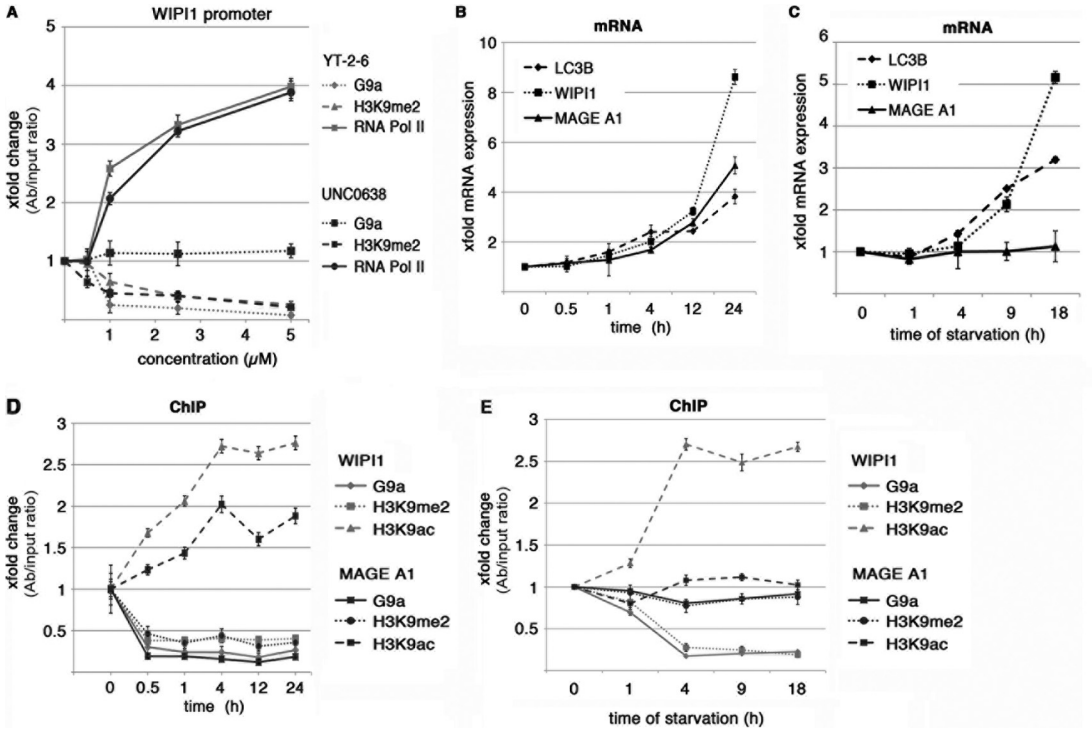

FIG 6 Nutrient deprivation leads to G9a-specific loss from autophagy gene promoters. (A) Quantitative ChIP PCR analysis for G9a association, H3K9me2, and RNA Pol II association with the WIPI1 promoter upon treatment with indicated concentrations of the G9a inhibitors YT-2-6 or UNC0638 for 24 h using primer P1. (B) Quantitative RT-PCR shows mRNA expression of LC3B, WIPI1, and MAGE A1 upon treatment with 3 μM YT-2-6 for the indicated times. Results were normalized to RPLP0 and are relative to diluent-treated cells (mean ± SD). (C) Quantitative RT-PCR shows mRNA expression of LC3B, WIPI1, and MAGE A1 upon glucose starvation for the indicated times. (D) Quantitative ChIP PCR analysis for G9a association, H3K9me2, and RNA Pol II association with the WIPI1 and MAGE A1 promoters upon treatment with 3 μM YT-2-6 for the indicated times using primer P1. (E) Quantitative ChIP PCR analysis for G9a association, H3K9me2, and RNA Pol II association with the WIPI1 and MAGE A1 promoters upon glucose starvation for indicated times using primer P1. Results in panels A, D, and E were normalized to input and are relative to diluent-treated cells (mean ± SD).

G9a is regulated during physiologic induction of autophagy. We next investigated the role of G9a during exposure to two physiologic stimuli that induce autophagy. Nutrient starvation leads to inhibition of mTORC1 and as a consequence triggers autophagy induction. As expected, upon starvation, we detected an increase in LC3B protein expression and lipidation (Fig. 5A), which was reflected by an increase in mRNA expression of LC3B, as well as an increase in DOR and WIPI1 mRNAs (Fig. 5B). G9a association with LC3B, WIPI1, and DOR promoters was diminished following starvation (Fig. 5C), which was accompanied by a reduction of H3K9me2 (Fig. 5D) and increased RNA polymerase II binding (Fig. 5E).

The specificity of the LC3B, WIPI1, and DOR promoter regulation by G9a is outlined by time course experiments comparing drug-related effects and starvation-related effects on marker gene expression. Pharmacologic inhibition of G9a leads to a significant reduction in both G9a binding and H3K9me2 at the WIPI1 promoter in a dose-dependent manner (Fig. 6A). G9a inhibitor treatment increased expression of G9a target genes which were related (LC3B and WIPI1) or not related (MAGE A1) to autophagy after 1 to 4 h posttreatment (Fig. 6B). In contrast, nutrient starvation resulted only in increased expression of the autophagy-related genes (LC3B and WIPI1), while MAGE A1 expression was unchanged (Fig. 6C). Consistent with the mRNA expression, G9a was removed from the WIPI1 and MAGE A1 promoters 30 min after treatment with the G9a inhibitor, with subsequent changes of the related histone marks (Fig. 6D). However, nutrient starvation resulted only in G9a removal from the WIPI1 promoter with subsequent reduction in the repressive H3K9me2 and increase of the activating H3K9ac mark, while the MAGE A1 promoter remained repressed (Fig. 6E). Taken together, these data suggest that starvation-induced autophagy leads to inhibition of G9a-mediated repression at the promoters of genes involved in autophagy.

In naive human $CD4^+$ T cells, for which the regulation of autophagy is an integral part of the activation program (40), inhibition of G9a led to LC3B-II induction in a dose-dependent manner (Fig. 7A). Moreover, CD3+CD28 stimulation of naive $CD4^+$ T cells strongly induced LC3B-II conversion as well as increasing mRNA expression of LC3B, WIPI1, and DOR (Fig. 7B and C). We also found that G9a association with the LC3B, WIPI1, and DOR promoters was diminished following activation of naive $CD4^+$ T cells (Fig. 7D and E). Loss of G9a was followed by reduced H3K9me2 (Fig. 7F), increased H3K9ac (Fig. 7G), and increased RNA polymerase II association (Fig. 7H) at all three promoters. While G9a was removed from its binding sites on autophagy-related genes, G9a protein levels were modestly decreased during T-cell activation or upon pharmacological inhibition (Fig. 7I). Taken together, these data indicate that G9a-mediated gene repression is specifically reversed by physiologic stimuli that induce autophagy.

JNK activity is required to inhibit G9a-mediated repression of autophagy genes following naive-T-cell stimulation. Multiple

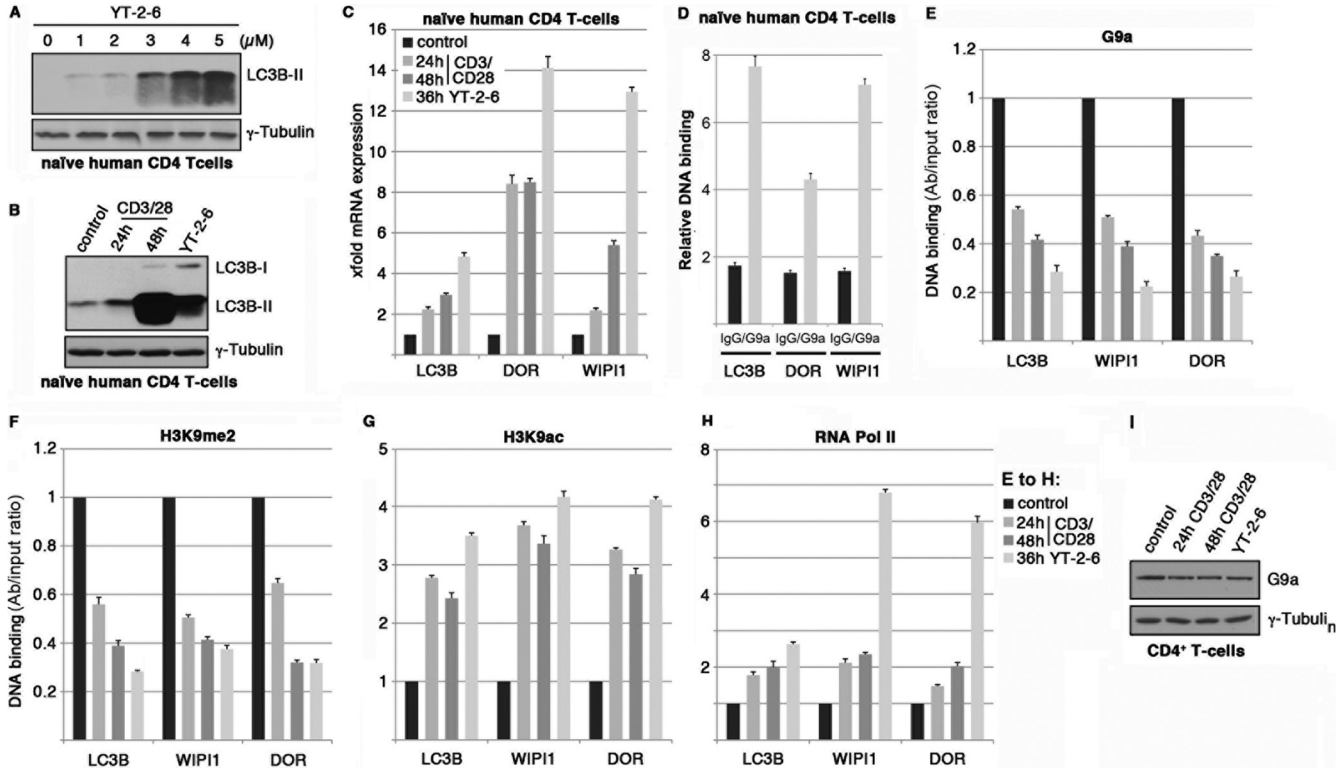

FIG 7 Naive-T-cell activation leads to G9a-dependent epigenetic changes at autophagy-related target gene promoters. (A and B) Immunoblot analysis shows expression and lipidation of LC3B in naive human CD4 T cells treated with increasing amounts of YT-2-6 for 24 h (A) or stimulated with anti-CD3/CD28 for 24 h and 48 h or treated with 3 μM YT-2-6 for 24 h (B). (C) Quantitative RT-PCR analysis of selected genes in naive human CD4 T cells stimulated with anti-CD3/CD28 for 24 h and 48 h or treated with 3 μM YT-2-6 for 36 h. (D) Quantitative PCR of ChIP analysis shows G9a association in naive human T cells with the LC3B, WIPI1, or DOR promoter relative to input and displayed as *x*-fold over the value for IgG (mean plus SD). (E to H) Quantitative PCR of ChIP analysis in naive human T cells stimulated with anti-CD3/CD28 for 24 h and 48 h or treated with 3 μM YT-2-6 for 36 h shows association of G9a (E), H3K9me2 (F), H3K9ac (G), and RNA polymerase II binding (H) to the LC3B, WIPI1, and DOR promoters. Results are relative to input and displayed as *x*-fold over the value for control cells (mean plus SD). Primer P1 for G9a, H3K9me2, and RNA Pol II and primer P2 for H3K9ac (see the cartoon in Fig. 4A) were used. (I) Immunoblot showing the levels of G9a after activation of naive T cells.

intracellular signaling pathways are engaged during T cell activation. The Src family kinase LCK is the proximal kinase that links TCR and CD28 signaling to downstream biochemical pathways required for cellular activation, including MEK, c-Jun N-terminal kinase (JNK), phosphatidylinositol 3-kinase (PI3K), phospholipase Cγ1, and protein kinase C (PKC) family members. To begin to elucidate the signaling pathways that couple TCR and CD28 ligation to the removal of G9a and the induction of autophagy gene expression, we treated naive $CD4^+$ T cells with pharmacologic inhibitors of these key signaling pathways. As expected, both LC3B and p62 gene expression were significantly increased following the stimulation of naive $CD4^+$ T cells treated with DMSO but not when cells were treated with the Src family kinase inhibitor protein phosphatase 2 (PP2) (Fig. 8A). Interestingly, treatment with either the MEK inhibitor (U0126) or JNK inhibitor (SP600125) but not inhibitors of PI3K, PKC family members, or PLCγ1 impaired LC3B and p62 gene expression (Fig. 8A) (our unpublished observations). Consistent with the gene expression, CD3-CD28-stimulated naive $CD4^+$ T cells showed increased protein expression of both p62 and LC3B-I as well as the generation of LC3B-II, both of which were prevented by pretreatment with either PP2 or the JNK inhibitor (JNKi) (Fig. 8B). Moreover, ChIP experiments demonstrated that the loss of G9a and H3K9me2 at the LC3B and p62 promoters was dependent on LCK and JNK activity (Fig. 8C). Lastly, as c-Jun is a known target of JNK in T cells, we examined the association of c-Jun with the LC3B and p62 promoters. As can be seen in Fig. 8D, upon stimulation of naive $CD4^+$ T cells, c-Jun binding is substantially increased at both promoters, and this induced association is prevented when either LCK or JNK is inhibited. Taken together, these data suggest that MEK- and JNK-regulated pathways are involved in coupling naive-T-cell activation to the expression of LC3B and SQSTM1. Moreover, our data suggest that c-Jun is recruited to the LC3B and p62 promoters in response to T cell activation, where it might participate in transcriptional regulation of these genes.

DISCUSSION

Herein, we show that the histone methyltransferase G9a represses the expression of genes involved in the autophagic process. Interestingly, pharmacologic inhibition or genetic depletion of G9a leads to the formation of LC3B-II, the aggregation of p62 and the formation of autophagosome-like structures. Moreover, our data suggest that in addition to cellular and transcriptional regulation of the autophagic process, G9a represses the expression of genes involved in autophagosome maturation under normal growth conditions. However, upon being subjected to physiologic stimuli that induce autophagy, such as starvation or activation of naive T

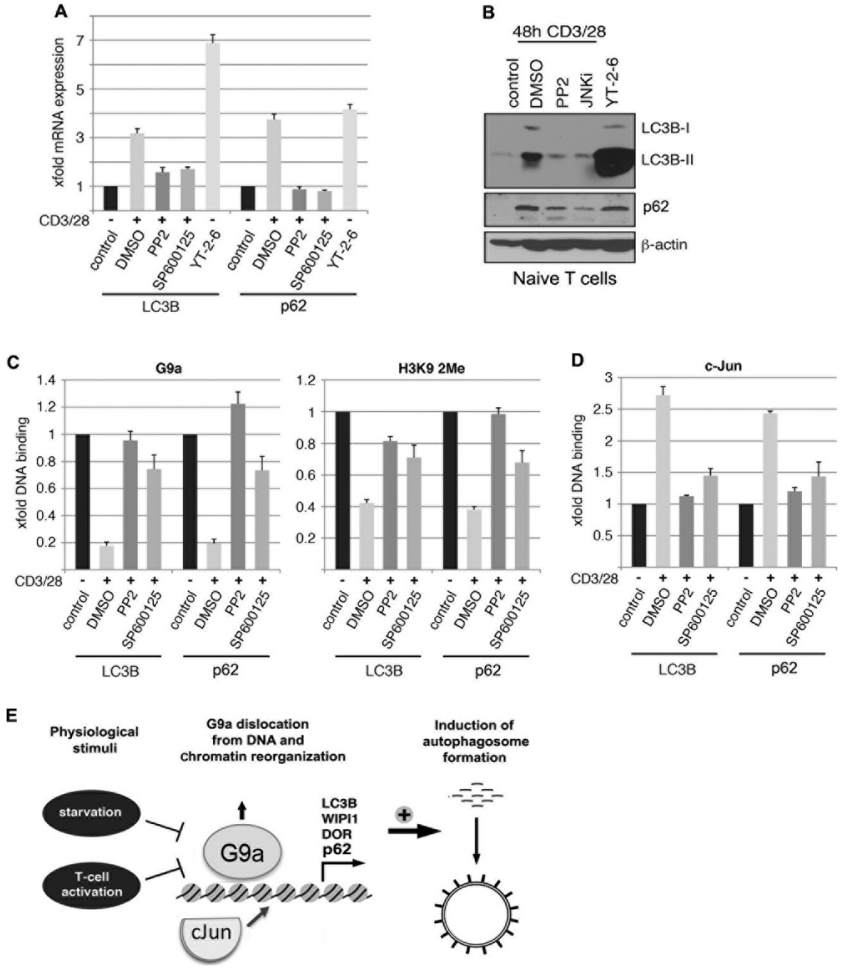

FIG 8 JNK activity is required for autophagy gene expression following the stimulation of naive $CD4^+$ T cells. (A) Quantitative RT-PCR for LC3B and p62 expression in naive human $CD4^+$ T cells stimulated with anti-CD3/CD28 for 36 h and simultaneously treated with diluent (DMSO), PP2 (2 μM), SP600125 (25 μM), or YT-2-6 (3 μM). Results are displayed as relative to DMSO control and normalized to RPLP0 (mean plus SD). (B) Naive $CD4^+$ T cells were stimulated with anti-CD3/CD28 for 48 h and simultaneously treated with diluent (DMSO), PP2 (2 μM), SP600125 (25 μM), or YT-2-6 (3 μM). Cellular proteins were isolated and immunoblotted for the expression of LC3B and p62. (C) Quantitative PCR analysis for G9a and H3K9me2 ChIP at the LC3B and p62 promoters. Naive $CD4^+$ T cells were stimulated with anti-CD3/CD28 for 36 h and simultaneously treated with diluent (DMSO), PP2 (2 μM), or SP600125 (25 μM). (D) Quantitative PCR analysis for c-Jun ChIP at the LC3B and p62 promoters. Naive $CD4^+$ T cells were stimulated with anti-CD3/CD28 for 36 h and simultaneously treated with diluent (DMSO), PP2 (2 μM), or SP600125 (25 μM). Results in panels C and D were normalized to input and are relative to unstimulated control cells (mean plus SD). (E) Under basal conditions, G9a epigenetically represses the expression of LC3B, DOR, and WIPI1 through H3K9me2. However, following physiologic stimuli that induce macroautophagy (glucose starvation or T cell activation), G9a is removed from these gene promoters and silencing marks are lost from the indicated macroautophagy-related target genes. Acetylases, transcription factors, and RNA Pol II can then access these target gene promoters, resulting in increased transcription of these genes and sustained autophagosome formation.

cells, G9a is dissociated from specific target gene promoters, with subsequent dynamic regulation of the chromatin landscape—reduced histone H3K9me2 and increased histone H3K9ac—at these sites, leading to increased transcription of LC3B, WIPI1, DOR, and p62 to "feed" the autophagic process (Fig. 8E). Taken together, these data point to a role for epigenetic regulation of autophagy by G9a and suggest that pharmacologic manipulation of G9a, or other epigenetic regulators, could impact this important cell survival process.

mTORC1 inhibition represents a key node regulating the decision to undergo the process of autophagy. Interestingly, inhibition of G9a was sufficient to induce LC3B-II formation, as well as the aggregation of both LC3B and p62. However, in contrast to mTORC1 inhibition, which induces autophagic flux (as measured by LC3B-II or p62 turnover), inhibition of G9a alone did not result in p62 or LC3B-II (data not shown) turnover, as measured by immunoblotting or analyzing the eGFP-mCherry-p62 sensor. Surprisingly, autophagic flux downstream of G9a inhibition still required mTORC1 inhibition, suggesting that inhibiting mTORC1 delivers a signal that leads to completion of the autophagic process. We propose that in the absence of this signal, G9a depletion or pharmacologic inhibition results in the increased expression of genes involved in the autophagic process, resulting in the formation of aberrant autophagosome-like structures that cannot undergo normal autophagic flux. Thus, G9a inhibition could be used to identify the signal(s) following mTORC1 inhibition that promotes autophagic flux.

Previous studies have identified several transcriptional regula-

tors of the autophagic process (12–14, 41). We provide evidence that the TCR/CD28-stimulated signaling pathways that regulate the induction of autophagy gene expression involve both the Ras-mitogen-activated protein kinase and JNK signaling cascades. Moreover, we show that c-Jun is recruited to the LC3B and p62 promoters following naive-T-cell activation. Whether c-Jun is recruited to the promoters of other autophagy genes following T cell stimulation remains to be determined. Recently TFEB, a gene involved in lysosomal biogenesis was found to coordinate the autophagy process through the regulation of autophagy and lysosomal genes (12). Interestingly, TFEB phosphorylation at Ser^{142} by ERK2 and mTOCR1 inhibits its nuclear accumulation, thereby preventing transactivation of its target genes (12, 42). Significantly, expression of TFEB containing a S142A mutation led to its nuclear accumulation regardless of nutrient deprivation or inhibition of mTORC1 and ultimately resulted in an induction of the autophagic-lysosomal system showing increased numbers of autophagosomes, lysosomes, and autophagolysosomes (12). We also saw increased expression of autophagy genes in response to G9a inhibition, as well as the formation of autophagosomes and swollen lysosomes (data not shown), suggesting that G9a might also be involved in lysosomal biogenesis, but this remains to be determined. In addition to TFEB, JunB gene expression is rapidly induced during nutrient deprivation, and it was shown that JunB depletion induced autophagy independently of nutrient deprivation or pharmacologic inhibition of mTORC1, whereas JunB overexpression abrogated LC3B aggregation and the onset of autophagy (41). The ability of JunB to bind DNA was required to inhibit autophagy, thereby implicating gene expression as the mechanism by which it could suppress autophagy. It is of interest that JunB can function as a transcriptional repressor and, in several instances, JunB and c-Jun share binding sites (43). It is therefore tempting to speculate that under normal growth conditions, JunB and G9a are both bound at autophagy gene promoters and that under conditions that induce autophagy (nutrient deprivation or naive-T-cell activation), both proteins are displaced, allowing chromatin remodeling and the binding of transcriptional activators such as c-Jun and TFEB to sustain the autophagic process.

The induction of autophagy not only leads to the degradation of proteins and organelles to produce the necessary biosynthetic components for survival but also results in the degradation of proteins required to maintain this catabolic process (e.g., LC3B and p62). Thus, in order to sustain autophagy during prolonged periods of cellular stress, transcription of genes involved in this process needs to be increased. Consistent, with this, we show that G9a is bound at the promoters of the LC3B, DOR, and WIPI1 genes and that upon starvation or stimulation of naive T cells, G9a and its repressive marks are removed to allow increased expression of these genes that will be utilized to sustain autophagy. Interestingly, G9a regulation of autophagy genes may be evolutionarily conserved, as several of the genes we found to be induced following G9a inhibition were also identified in *Drosophila melanogaster* following ChIP-Seq for G9a-regulated genes (38). Moreover, the loss of G9a from the LC3B, DOR, and WIPI1 promoters in response to autophagy induction appears to be gene and/or promoter specific, as neither G9a binding nor H3K9me2 was removed from the well-established G9a target MAGE A1. This is an important observation, as it suggests that there is sequence-specific inactivation of G9a and not just a global loss of G9a-mediated repression in response to nutrient deprivation. Clearly, the identification of additional transcriptional repressors, including transcription factors and other epigenetic modifiers, will provide further insight into how these genes are specifically regulated during autophagy induction. Lastly, our study supports and extends recent findings of G9a-dependent simultaneous decrease of H3K9me2 and increase of H3K9ac (44) and links this type of regulation to autophagy.

In conclusion, our data identify G9a as an epigenetic regulator of autophagy that participates in the repression of key genes involved in autophagosome formation under normal growth conditions. Future work aimed at understanding the sequence-specific recruitment of G9a to these promoter elements, as well as the identification of the signaling pathways engaged by starvation that lead to G9a removal from the promoters and the subsequent epigenetic changes which drive gene expression, will be important. Uncovering these pathways could reveal novel therapeutic targets to either enhance or prevent the induction of autophagy.

ACKNOWLEDGMENTS

This study was supported in part by the Mayo Foundation for Medical Research. D.D.B. was supported by NCI-funded Pancreatic Cancer SPORE grant CA102701. A.K. was supported by a Mildred-Scheel fellowship of the Deutsche Krebshilfe (no. 109294). M.H.V. was supported by Universidad del Pais Vasco, Instituto Biodonostia, San Sebastian, Spain, and CIBERehd (red de enfermedades hepaticas y digestivas). V.E. was supported by Deutsche Forschungsgemeinschaft (KF0210, SFB-TR17, and German Cancer Research Foundation no. 109423). NIGMS GM097057 was awarded to D.H.K.

We have no conflicts of interest to declare.

REFERENCES

1. **Klionsky DJ.** 2007. Autophagy: from phenomenology to molecular understanding in less than a decade. Nat. Rev. Mol. Cell Biol. **8:**931–937.
2. **Mehrpour M, Esclatine A, Beau I, Codogno P.** 2010. Overview of macroautophagy regulation in mammalian cells. Cell Res. **20:**748–762.
3. **Johansen T, Lamark T.** 2011. Selective autophagy mediated by autophagic adapter proteins. Autophagy **7:**279–296.
4. **Fimia GM, Kroemer G, Piacentini M.** 2013. Molecular mechanisms of selective autophagy. Cell Death Differ. **20:**1–2.
5. **Choi AMK, Ryter SW, Levine B.** 2013. Autophagy in human health and disease. N. Engl. J. Med. **368:**651–662.
6. **Tsukada M, Ohsumi Y.** 1993. Isolation and characterization of autophagy-defective mutants of Saccharomyces cerevisiae. FEBS Lett. **333:** 169–174.
7. **Mauthe M, Jacob A, Freiberger S, Hentschel K, Stierhof Y-D, Codogno P, Proikas-Cezanne T.** 2011. Resveratrol-mediated autophagy requires WIPI-1-regulated LC3 lipidation in the absence of induced phagophore formation. Autophagy **7:**1448–1461.
8. **Mauthe M, Yu W, Krut O, Krönke M, Götz F, Robenek H, Proikas-Cezanne T.** 2012. WIPI-1 positive autophagosome-like vesicles entrap pathogenic Staphylococcus aureus for lysosomal degradation. Int. J. Cell Biol. **2012:**179207.
9. **Mauvezin C, Orpinell M, Francis VA, Mansilla F, Duran J, Ribas V, Palacín M, Boya P, Teleman AA, Zorzano A.** 2010. The nuclear cofactor DOR regulates autophagy in mammalian and Drosophila cells. EMBO Rep. **11:**37–44.
10. **Sancho A, Duran J, García-España A, Mauvezin C, Alemu EA, Lamark T, Macias MJ, DeSalle R, Royo M, Sala D, Chicote JU, Palacín M, Johansen T, Zorzano A.** 2012. DOR/Tp53inp2 and Tp53inp1 constitute a metazoan gene family encoding dual regulators of autophagy and transcription. PLoS One **7:**e34034. doi:10.1371/journal.pone.0034034.
11. **Codogno P, Mehrpour M, Proikas-Cezanne T.** 2012. Canonical and non-canonical autophagy: variations on a common theme of self-eating? Nat. Rev. Mol. Cell Biol. **13:**7–12.
12. **Settembre C, Di Malta C, Polito VA, Garcia Arencibia M, Vetrini F, Erdin S, Erdin SU, Huynh T, Medina D, Colella P, Sardiello M,**

Rubinsztein DC, Ballabio A. 2011. TFEB links autophagy to lysosomal biogenesis. Science **332:**1429–1433.
13. **Polager S, Ofir M, Ginsberg D.** 2008. E2F1 regulates autophagy and the transcription of autophagy genes. Oncogene **27:**4860–4864.
14. **Juhász G, Puskás LG, Komonyi O, Erdi B, Maróy P, Neufeld TP, Sass M.** 2007. Gene expression profiling identifies FKBP39 as an inhibitor of autophagy in larval Drosophila fat body. Cell Death Differ. **14:**1181–1190.
15. **Esteller M.** 2008. Epigenetics in cancer. N. Engl. J. Med. **358:**1148–1159.
16. **Chen MW, Hua KT, Kao HJ, Chi CC, Wei LH, Johansson G, Shiah SG, Chen PS, Jeng YM, Cheng TY, Lai TC, Chang JS, Jan YH, Chien MH, Yang CJ, Huang MS, Hsiao M, Kuo ML.** 2010. H3K9 histone methyltransferase G9a promotes lung cancer invasion and metastasis by silencing the cell adhesion molecule Ep-CAM. Cancer Res. **70:**7830–7840.
17. **Huang J, Dorsey J, Chuikov S, Pérez-Burgos L, Zhang X, Jenuwein T, Reinberg D, Berger SL.** 2010. G9a and Glp methylate lysine 373 in the tumor suppressor p53. J. Biol. Chem. **285:**9636–9641.
18. **Kondo Y, Shen L, Ahmed S, Boumber Y, Sekido Y, Haddad BR, Issa J-PJ.** 2008. Downregulation of histone H3 lysine 9 methyltransferase G9a induces centrosome disruption and chromosome instability in cancer cells. PLoS One **3:**e2037. doi:10.1371/journal.pone.0002037.
19. **Kondo Y, Shen L, Suzuki S, Kurokawa T, Masuko K, Tanaka Y, Kato H, Mizuno Y, Yokoe M, Sugauchi F, Hirashima N, Orito E, Osada H, Ueda R, Guo Y, Chen X, Issa J-PJ, Sekido Y.** 2007. Alterations of DNA methylation and histone modifications contribute to gene silencing in hepatocellular carcinomas. Hepatol. Res. **37:**974–983.
20. **Duan Z, Zarebski A, Montoya-Durango D, Grimes HL, Horwitz M.** 2005. Gfi1 coordinates epigenetic repression of p21Cip/WAF1 by recruitment of histone lysine methyltransferase G9a and histone deacetylase 1. Mol. Cell. Biol. **25:**10338–10351.
21. **Nishio H, Walsh MJ.** 2004. CCAAT displacement protein/cut homolog recruits G9a histone lysine methyltransferase to repress transcription. Proc. Natl. Acad. Sci. U. S. A. **101:**11257–11262.
22. **Tachibana M, Sugimoto K, Nozaki M, Ueda J, Ohta T, Ohki M, Fukuda M, Takeda N, Niida H, Kato H, Shinkai Y.** 2002. G9a histone methyltransferase plays a dominant role in euchromatic histone H3 lysine 9 methylation and is essential for early embryogenesis. Genes Dev. **16:**1779–1791.
23. **Smallwood A, Estève P-O, Pradhan S, Carey M.** 2007. Functional cooperation between HP1 and DNMT1 mediates gene silencing. Genes Dev. **21:**1169–1178.
24. **Estève P-O, Chin HG, Smallwood A, Feehery GR, Gangisetty O, Karpf AR, Carey MF, Pradhan S.** 2006. Direct interaction between DNMT1 and G9a coordinates DNA and histone methylation during replication. Genes Dev. **20:**3089–3103.
25. **Zhang J, Gao Q, Li P, Liu X, Jia Y, Wu W, Li J, Dong S, Koseki H, Wong J.** 2011. S phase-dependent interaction with DNMT1 dictates the role of UHRF1 but not UHRF2 in DNA methylation maintenance. Cell Res. **21:**1723–1739.
26. **Gomez TS, Billadeau DD.** 2009. A FAM21-containing WASH complex regulates retromer-dependent sorting. Dev. Cell **17:**699–711.
27. **Vedadi M, Barsyte-Lovejoy D, Liu F, Rival-Gervier S, Allali-Hassani A, Labrie V, Wigle TJ, DiMaggio PA, Wasney GA, Siarheyeva A, Dong A, Tempel W, Wang S-C, Chen X, Chau I, Mangano TJ, Huang X-P, Simpson CD, Pattenden SG, Norris JL, Kireev DB, Tripathy A, Edwards A, Roth BL, Janzen WP, Garcia BA, Petronis A, Ellis J, Brown PJ, Frye SV, Arrowsmith CH, Jin J.** 2011. A chemical probe selectively inhibits G9a and GLP methyltransferase activity in cells. Nat. Chem. Biol. **7:**566–574.
28. **Egan DF, Shackelford DB, Mihaylova MM, Gelino S, Kohnz RA, Mair W, Vasquez DS, Joshi A, Gwinn DM, Taylor R, Asara JM, Fitzpatrick J, Dillin A, Viollet B, Kundu M, Hansen M, Shaw RJ.** 2011. Phosphorylation of ULK1 (hATG1) by AMP-activated protein kinase connects energy sensing to mitophagy. Science **331:**456–461.
29. **Kim J, Kundu M, Viollet B, Guan K-L.** 2011. AMPK and mTOR regulate autophagy through direct phosphorylation of Ulk1. Nat. Cell Biol. **13:**132–141.
30. **Shang L, Chen S, Du F, Li S, Zhao L, Wang X.** 2011. Nutrient starvation elicits an acute autophagic response mediated by Ulk1 dephosphorylation and its subsequent dissociation from AMPK. Proc. Natl. Acad. Sci. U. S. A. **108:**4788–4793.
31. **Habib SL, Kasinath BS, Arya RR, Vexler S, Velagapudi C.** 2010. Novel mechanism of reducing tumourigenesis: upregulation of the DNA repair enzyme OGG1 by rapamycin-mediated AMPK activation and mTOR inhibition. Eur. J. Cancer **46:**2806–2820.
32. **Mizushima N, Yamamoto A, Hatano M, Kobayashi Y, Kabeya Y, Suzuki K, Tokuhisa T, Ohsumi Y, Yoshimori T.** 2001. Dissection of autophagosome formation using Apg5-deficient mouse embryonic stem cells. J. Cell Biol. **152:**657–668.
33. **Hanada T, Noda NN, Satomi Y, Ichimura Y, Fujioka Y, Takao T, Inagaki F, Ohsumi Y.** 2007. The Atg12-Atg5 conjugate has a novel E3-like activity for protein lipidation in autophagy. J. Biol. Chem. **282:**37298–37302.
34. **Bjørkøy G, Lamark T, Pankiv S, Øvervatn A, Brech A, Johansen T.** 2009. Monitoring autophagic degradation of p62/SQSTM1. Methods Enzymol. **452:**181–197.
35. **Pankiv S, Clausen TH, Lamark T, Brech A, Bruun J-A, Outzen H, Øvervatn A, Bjørkøy G, Johansen T.** 2007. p62/SQSTM1 binds directly to Atg8/LC3 to facilitate degradation of ubiquitinated protein aggregates by autophagy. J. Biol. Chem. **282:**24131–24145.
36. **Itakura E, Mizushima N.** 2011. p62 Targeting to the autophagosome formation site requires self-oligomerization but not LC3 binding. J. Cell Biol. **192:**17–27.
37. **Proikas-Cezanne T, Robenek H.** 2011. Freeze-fracture replica immunolabelling reveals human WIPI-1 and WIPI-2 as membrane proteins of autophagosomes. J. Cell. Mol. Med. **15:**2007–2010.
38. **Kramer JM, Kochinke K, Oortveld MAW, Marks H, Kramer D, de Jong EK, Asztalos Z, Westwood JT, Stunnenberg HG, Sokolowski MB, Keleman K, Zhou H, van Bokhoven H, Schenck A.** 2011. Epigenetic regulation of learning and memory by Drosophila EHMT/G9a. PLoS Biol. **9:**e1000569. doi:10.1371/journal.pbio.1000569.
39. **Yokochi T, Poduch K, Ryba T, Lu J, Hiratani I, Tachibana M, Shinkai Y, Gilbert DM.** 2009. G9a selectively represses a class of late-replicating genes at the nuclear periphery. Proc. Natl. Acad. Sci. U. S. A. **106:**19363–19368.
40. **Walsh CM, Bell BD.** 2010. T cell intrinsic roles of autophagy in promoting adaptive immunity. Curr. Opin. Immunol. **22:**321–325.
41. **Yogev O, Goldberg R, Anzi S, Yogev O, Shaulian E.** 2010. Jun proteins are starvation-regulated inhibitors of autophagy. Cancer Res. **70:**2318–2327.
42. **Settembre C, Zoncu R, Medina DL, Vetrini F, Erdin S, Erdin S, Huynh T, Ferron M, Karsenty G, Vellard MC, Facchinetti V, Sabatini DM, Ballabio A.** 2012. A lysosome-to-nucleus signalling mechanism senses and regulates the lysosome via mTOR and TFEB. EMBO J. **31:**1095–1108.
43. **Shaulian E.** 2010. AP-1—the Jun proteins: oncogenes or tumor suppressors in disguise? Cell. Signal. **22:**894–899.
44. **Qiang M, Denny A, Lieu M, Carreon S, Li J.** 2011. Histone H3K9 modifications are a local chromatin event involved in ethanol-induced neuroadaptation of the NR2B gene. Epigenetics **6:**1095–1104.